

Active Site Protonation of 1-Azafagomine in Glucosidases Studied by Solid-State NMR Spectroscopy

Astrid C. Sivertsen,^[a] Magdalena Gasior,^[a] Morten Bjerring,^[a] Steen U. Hansen,^[a] Oscar Lopez Lopez,^[a] Niels C. Nielsen,^{*[a]} and Mikael Bols^{*[a]}

Keywords: Azasugars / Carbohydrates / Inhibitors / Enzymes / Molecular recognition

Protonation of an azasugar inhibitor inside the active site of a glycosidase has been studied by solid-state NMR spectroscopy. By measuring ¹³C chemical shifts of azafagomine bound to yeast α -glucosidase, almond β -glucosidase, and *Aspergillus niger* glucoamylase, and ¹⁵N chemical shift of azafagomine bound to β -glucosidase, we find evidence for an N1-protonation of azafagomine inside β -glucosidase. For

α -glucosidase and glucoamylase the corresponding chemical shifts are similar to those of the non-protonated inhibitor, which shows that charge stabilization at anomeric position is not occurring in these enzymes.

(© Wiley-VCH Verlag GmbH & Co. KGaA, 69451 Weinheim, Germany, 2007)

Introduction

Carbohydrates linked to proteins and lipids are ubiquitous in biology. For example, they fine-tune the processes of self and non-self distinction, cancer metastasis, inflammatory and immune response such as diabetes, and the ability of HIV, Hepatitis and other vira to assemble and bud from host cells. The emerging field of glycobiology uses carbohydrate-structures as vaccines against carbohydrate-binding proteins and carbohydrate-processing enzymes.^[1] There is a great interest in elucidating the regulatory mechanism of such enzymes, which typically involve specific ligand binding. Understanding what happens to inhibitors upon active-site binding in terms of structural and conformational changes, charge dislocation, and protonation is regarded an important step towards understanding enzymatic reaction mechanisms. With the general belief that a central element in enzymatic catalysis is the ability of the enzyme to lower the energy of the transition state for the catalyzed reaction,^[2] much effort has been devoted to design of compounds that resemble the expected transition state of glycoside cleavage in terms of polarity and shape to create potent enzyme inhibitors.

1-Azasugars, characterized by having a nitrogen in place of anomeric carbon, and iminosugars, characterized by having a nitrogen in place of ring-oxygen, range among the most potent inhibitors of glycosidases and related enzymes.^[3,4] These inhibitors have often been considered transition-state analogues of glycoside cleavage^[5,6] since they in

protonated form mimic the charge of oxocarbenium ion or carbocation transition states.

However, despite the fact that the protonation states are critical to the interpretation of inhibitor strength very little is known about them. Inhibition profiles as a function of pH are ambiguous because they show a combination of the protonation behaviour of free enzyme, inhibitor and complex' pK_a values. Direct observation of protonation states is therefore necessary. This is, however, not trivial. Davies and collaborators have used atomic-resolution X-ray crystallography to study complexes of several basic inhibitors in glycosidases.^[7] They showed that 4-*O*-(β -D-glu)-isofagomine, an 1-azasugar, was protonated in the active site of endocellulase Cel5A and bound to the dicarboxylate form of the enzyme (E).^[8] This result, protonated inhibitor (IH) binding to E, was consistent with the pH/K_i profile of the inhibitor. On this basis Davies concluded that this isofagomine could not be a transition state analogue since it did not bind to the catalytic form of the enzyme.^[8] On the other hand, in two other complexes between xylanase Xyn10A and 4-*O*-(β -D-xy)-D-xylo-1-deoxynojirimycin or 4-*O*-(β -D-xy)-D-xylo-isofagomine protonation states could not be determined despite atomic resolution.^[9] At present the protonation states of iminosugars have not been reported.

¹³C or ¹⁵N cross-polarization (CP) magic-angle-spinning (MAS) solid state NMR of inhibitor complexes using ¹³C or ¹⁵N labelled inhibitors are methods that may be used to study protonation states of bound glycosidase inhibitors. Although several isotope labelled glycosidase inhibitors (Figure 1) have been reported no such study has apparently been made. In this area of research, Vasella and collaborators prepared a ¹⁵N labelled glucoimidazol and used it to distinguish tautomeric forms,^[10] and Stütz et al. have prepared a ¹³C-labelled 1-deoxynojirimycin.^[11]

[a] Center for Insoluble Protein Structures (inSPIN), Interdisciplinary Nanoscience Center (iNANO) and Department of Chemistry, University of Aarhus, 8000 Aarhus, Denmark

Supporting information for this article is available on the WWW under <http://www.eurjoc.org> or from the author.

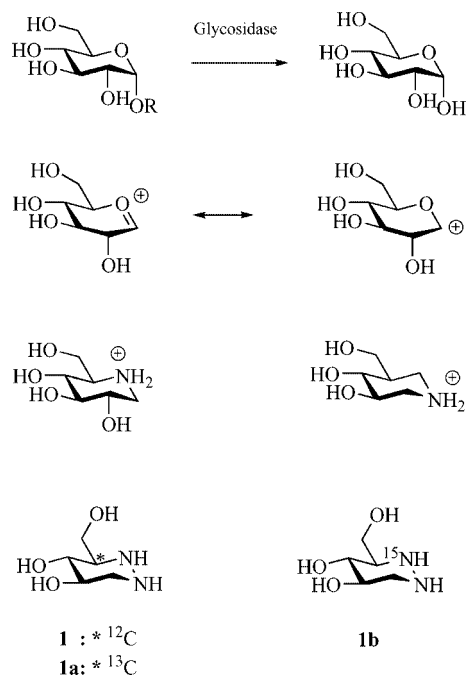


Figure 1. Glycoside hydrolysis transition states and glycosidase inhibitors.

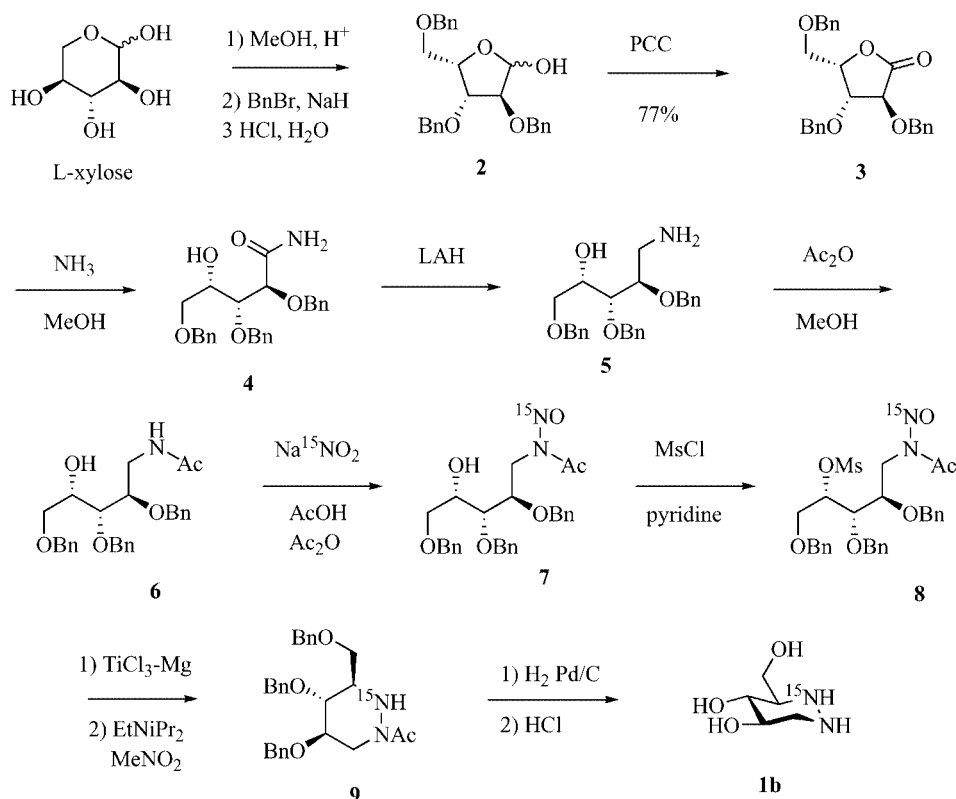
In the present work, it was the intention to see whether NMR could be used to give insight into this problem and reveal protonation states of nitrogen containing glycosidase inhibitors. These protonation states would have an influence on the transition state mimicry of such inhibitors. We

chose in this study the glycosidase inhibitor, 1-azafagomine (**1**) for several reasons: 1) It is a potent inhibitor (K_i 0.1–10 μM) of both α - and β -glycosidases.^[12,13] 2) It has a low pK_a value making it largely unprotonated at assay conditions. This has the advantage that protonation under these conditions is unlikely unless being induced specifically by the enzyme. 3) It has two protonation sites, either at a pseudo-anomeric position or at a pseudo-ring oxygen position. This means that this compound may reveal information about an enzyme's preference for protonation. It also means that this compound potentially can act as a "stand-in" for both 1-azasugar and iminosugar glycosidase inhibitors.

In the present work we report the synthesis of **1b**, a ^{15}N -labelled version of **1**, and the results of ^{13}C - and ^{15}N (CP/MAS) solid-state NMR with this and 3- ^{13}C -labelled **1a** bound to some glycosidases. The results of the study are not conclusive, but suggest that **1a** is protonated in the active site of β -glucosidase and neutrally bound in α -glucosidase and glucoamylase.

Results and Discussion

Synthesis. Compounds **1** and (\pm)-**1a** were prepared as previously reported.^[13,15] Compound **1b**, a 2-(^{15}N)-labelled analogue of **1**, was prepared as outlined in Scheme 1. This synthesis is related to our original synthesis of **1**, but with the important difference that the N–N bond has to be synthesised to ensure control over the position of ^{15}N . So L-



Scheme 1. Synthesis of ^{15}N -labelled azafagomine **1b**.

xylose was converted into the tribenzylxylofuranose **2** as previously, but then oxidised to the lactone **3** using PCC. The lactone was treated with ammonia in methanol to give the amide **4** in 99% yield, which was reduced with LAH to give the amine **5** in 86% yield. This two-step protocol for reaching **5** from **3** is much better than reductive amination of **3**, which if carried out with ammonia leads to a significant amount of overalkylation, and when done with primary amines, like allylamine and *p*-methoxybenzylamine, necessitates some troublesome deprotection chemistry at N. Compound **5** was acetylated with acetic anhydride in methanol to give *N*-acetamide **6** in 90% yield.

Now introduction of ^{15}N was carried out by nitrosation of the amide **6** using $\text{Na}^{15}\text{NO}_2$ in a mixture of acetic acid and acetic anhydride giving the *N*-nitroso compound **7** in 77% yield. The unprotected alcohol was mesylated with mesyl chloride in pyridine giving **8** in 89% yield. Selective reduction of the *N*-nitroso function to a hydrazine, a rather tricky reaction, was realised with TiCl_3/Mg to give a product that was immediately cyclised with base to give **9** in 53% yield over the two steps. The final two deprotection steps, hydrogenolysis and acidic hydrolysis, followed the previous synthesis of **1** and gave a 59% yield of **1b**, having the expected mass and a ^{15}N NMR chemical shift of 83.1 ppm.

Inhibition profile of 1 as a function of pH. At a series of different pH, we measured the $k_{\text{cat}}/K_{\text{m}}$ and the K_{i} values for the inhibition by **1** of yeast α -glucosidase (see Figure 2 and S1 in the supporting information) and almond β -glucosidase (Figure 3 and S2) obtaining relationships that reflect protonation changes in inhibitor and enzyme active site. From the $k_{\text{cat}}/K_{\text{m}}$ curve (see supporting information) it is seen that the α -enzyme has a pH optimum of 6.1, and that the $\text{p}K_{\text{a}}$ values of the protonating and nucleophilic carboxylate residues in its active site are 5.5 and 6.7, respectively. The inhibition profile for **1** with the α -glucosidase is sigmoid shaped with a pH optimum at 6.3, and an observed optimum K_{i} of $3.6 \mu\text{M}$. A simulation using the $\text{p}K_{\text{a}}$ values of 5.5 and 6.7 for the enzyme and 5.3 for **1** shows that this inhibition behaviour fits well with either **1** binding to monoprotonated enzyme (EH) or protonated **1** (1H^+) binding to unprotonated enzyme (E). In the former case the real

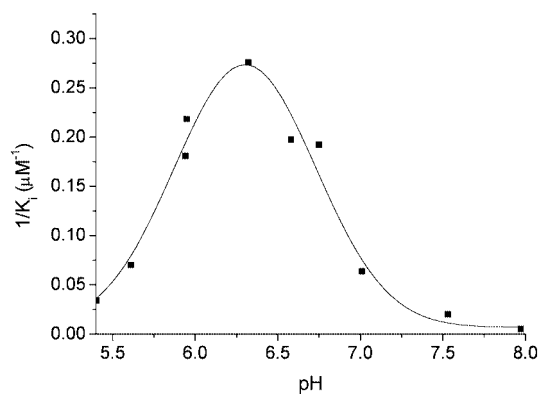


Figure 2. Curve of $1/K_{\text{i}}$ for inhibition of yeast α -glucosidase by **1** as a function of pH.

$K_{\text{i}}(\text{real}) = \text{E}^*\text{1H}^+/\text{EI}$ becomes $2.1 \mu\text{M}$, while the latter case $K_{\text{i}}(\text{real}) = \text{EH}^*\text{1}/\text{EI}$ becomes 84 nM . The curve is not compatible with 1H binding EH or **1** binding EH_2 .

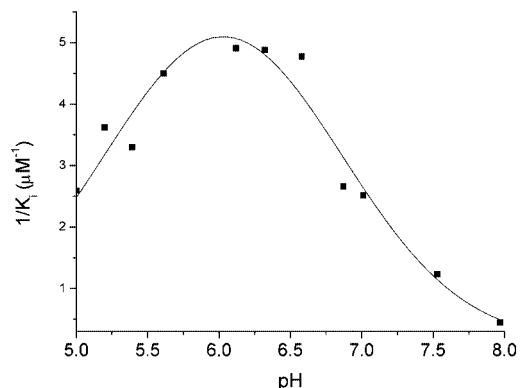


Figure 3. Curve of $1/K_{\text{i}}$ for inhibition of almond β -glucosidase by **1** as a function of pH.

For the β -glucosidase a similar relationship is found: Here the enzyme pH optimum was 5.75 with acidic and nucleophilic $\text{p}K_{\text{a}}$ values of 4.8 and 6.7. Azafagomine (**1**) inhibition has optimum at pH 6.0 and the observed K_{i} at this pH is $0.2 \mu\text{M}$. Again, both the case of **1** binding to EH or 1H^+ binding to E will theoretically fit this curve, when the above $\text{p}K_{\text{a}}$ values and the $\text{p}K_{\text{a}}$ of 5.3 for **1** is used in the calculation, while other possibilities, such as 1H binding EH or **1** binding EH_2 do not fit. In the case of **1** binding to EH the real $K_{\text{i}}(\text{real}) = \text{E}^*\text{1H}^+/\text{EI}$ becomes $0.13 \mu\text{M}$, while for 1H^+ binding to E the $K_{\text{i}}(\text{real}) = \text{EH}^*\text{1}/\text{EI}$ becomes 5.2 nM .

Study of binding of 1a. Firstly, we studied the binding of the inhibitor (\pm)-3-(^{13}C)-4,5-dihydroxy-3-(hydroxymethyl)-hexahydropyridazine^[15] (**1a**) to three different sugar-processing enzymes: yeast α -glucosidase, almond β -glucosidase, and *Aspergillus niger* glucoamylase.^[14] These enzymes were chosen because iminosugars are potent inhibitors of α -glucosidase, while 1-azasugars are potent inhibitors of β -glucosidase. It has been proposed that the charge development occurring in the α - and β -glucosidase transition states differs, with the former having oxocarbenium ion character and the latter carbocation character.^[6] As mentioned above, **1** inhibits all three enzymes and this may be due to the compound's ability to mimic several transition states by having two possible protonated forms. The large enzyme-inhibitor complexes tumble too slowly for detection of enzyme-bound **1a** using traditional liquid-state NMR experiments,^[15] (For some examples of protein-carbohydrate complexes that can be studied by NMR in solution, see ref.^[16,17]) and the exchange rate of the inhibitor between the free and enzyme-bound state is too slow for indirect observation of the bound inhibitor by means of transferred NOE experiments (data not shown). Solid-state NMR is not dependent on fast molecular tumbling, and is therefore applicable in investigation of these systems.

By appropriate tuning of the dipolar-coupling mediated ^1H to ^{13}C (or ^1H to ^{15}N) polarization transfer conditions relative to the molecular motion, CP/MAS solid-state

NMR offers the possibility to distinguish ligands in the binding site from those non-specifically bound to the enzyme or free in the solvent. In the present case, such conditions were met by freezing an aqueous solution of the enzyme with different amounts of ligand to $-42\text{ }^{\circ}\text{C}$ and using CP/MAS with 3.37 kHz spinning, 1 ms contact time, and 4 s relaxation delay. Specifically, the discrimination of signals from frozen non-bound ligands and enzyme-bound ligands was established by carefully optimizing the CP/MAS conditions at different temperatures for samples with and without enzyme present to make preference to signals from bound ligands. The discrimination of signals from bound and non-bound ligands was subsequently tested by titrating in excessive amounts of unlabelled ligand, where attenuation/elimination of the signal from the ^{13}C -labelled ligand in agreement with the number of binding sites verifies that it is not (or much less) observable under displaced (unbound) conditions.

In the ^{13}C CP/MAS spectra for β -glucosidase, the ligand displays a quite narrow resonance at $\delta = 60.2\text{ ppm}$ after addition of 1 equiv. of **1a** (Table 1). Upon further addition of 1 and 2 eqs. of ligand the overall intensity of the peak increases, as manifested by an increase in the peak height for the narrow resonance as well as an increase in the line width near the baseline. The latter contribution is attributed to **1a** non-specifically bound to β -glucosidase, while the narrow component is assigned to Figure 4. ^{13}C CP/MAS spectra of (a) yeast α -glucosidase, (b) almond β -glucosidase, and (c) *Aspergillus niger* glucoamylase with different amounts of **1a** and **1**. From bottom to top the spectra represent the enzyme (148, 126, 151 nmol in 60 μL H_2O) without **1a** and **1**, with ca. 1 equiv. **1a** (195, 105, 152 nmol), with ca. 2 equiv. **1a** (371, 268, – nmol), with ca. 3 equiv. **1a** (541, 473, 456 nmol), and ca. 3 equiv. **1a** plus 40–80 equiv. (7.4, 8.4, 12.2 mmol) of **1**. Left: the aliphatic region of the ^{13}C CP/MAS spectrum (5000–15000 scans). Right: difference between the spectrum to the left and the bottom left spectrum.

Table 1. ^{13}C chemical shifts (relative to external TMS) and binding constants for **1a** specifically bound to the three enzymes (see text). The K_i values are in μM at $25\text{ }^{\circ}\text{C}$, pH 6.8 and were taken from ref.^[12,13]

	β -Glucosidase	α -Glucosidase	Glucoamylase
K_i (μM)	0.33	6	10
Chemical shift (ppm)	60.2	62.7	63.0

1a in the inhibitor binding site. This interpretation is supported by further addition of 65 eqs. of **1**, which eliminates the narrow resonance by dilution of the ^{13}C labels in the binding site. Under the present experimental conditions ^{13}C signals from **1a** in the frozen solvent are excited much less efficiently than those for specific enzyme bound **1a** (and the non-bound are thereby invisible). Similarly, the spectra of **1a** bound to α -glucosidase and glucoamylase reveals ^{13}C resonances at $\delta = 62.7$ and 63.0 ppm , respectively, for specific bound **1a** (Table 1). For comparison the ^{13}C chemical shift of **1a** was 63.5 ppm in neutral solution and 61.7 ppm in acidic solution.

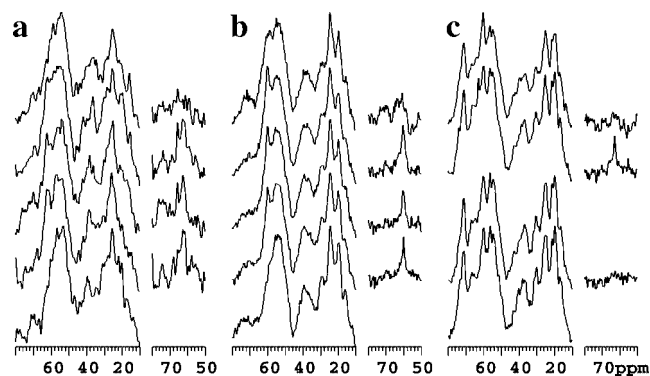


Figure 4. A series of ^{13}C CP/MAS spectra of α -glucosidase, β -glucosidase, and glucoamylase with different amounts of **1a**^[18,19] and **1**^[13] titrated into the solution prior to freezing. For each enzyme the lower row contains the relevant aliphatic region of the ^{13}C CP/MAS spectrum for the enzyme, while the four upwards following rows contain spectra for the enzyme upon addition of approx. 1, 2, and 3 equiv. of **1a**, and finally further 40–80 equiv. of **1**. To discriminate the ligand ^{13}C resonance from the large natural abundance ^{13}C background of the enzyme, we have for each enzyme included difference plots obtained by subtracting the pure enzyme spectrum (lower row) from the ligand-titrated spectra (left) to the right of each spectrum in Figure 4.

Study of binding of 1b. The chemical shifts of the two nitrogen sites in **1b** were measured in neutral and acidic solution (see Table 2).

Table 2. ^{15}N chemical shifts (relative to external liq. NH_3) of **1b** in neutral and acidic solution.

	Chemical shift (ppm)	
	1- ^{15}N	2- ^{15}N
Neutral	77.2	85.3
Acidic	73.8	84.9

The binding of the inhibitor 2-(^{15}N)-4,5-dihydroxy-3-(hydroxymethyl)hexahydropyridazine (**1b**) to β -glucosidase was studied by various solid-state NMR methods. Figure 5 shows a ^{15}N CP/MAS NMR spectrum of a **1b**- β -glucosidase complex at $-21\text{ }^{\circ}\text{C}$, displaying a broad signal at 110–130 ppm which is assigned to natural abundance backbone amides of the enzyme, and a single signal at $\delta = 82.6\text{ ppm}$, which is assigned to isotope labeled 2- ^{15}N site from specifically bound **1b**. It is noted that the two signals have a 3:1 relationship in intensities, as would be expected based on a 67 kDa molecular weight of β -glucosidase, combined with 0.37% natural abundance of ^{15}N , and a 1:0.9 molar ratio of enzyme and inhibitor in the sample.

To further explore the protonation properties of the nitrogens, ^{15}N cross-polarization depolarization (CPD) experiments^[20] were carried out on ^{15}N -*t*Boc-valine (included as a control as it is known to contain an NH group), free **1b**, and the **1b**- β -glucosidase complex, shown in Figure 6. The data were fit to Equation (1) for an NH group and Equation (2) for an NH_2 group, where T_d is a time constant that describes magnetization decay caused by spin diffusion between directly bonded and more distant protons, T_2 describes decay caused by direct dipolar coupling between ^1H and ^{15}N , and τ_2 is depolarization period of the CPD experi-

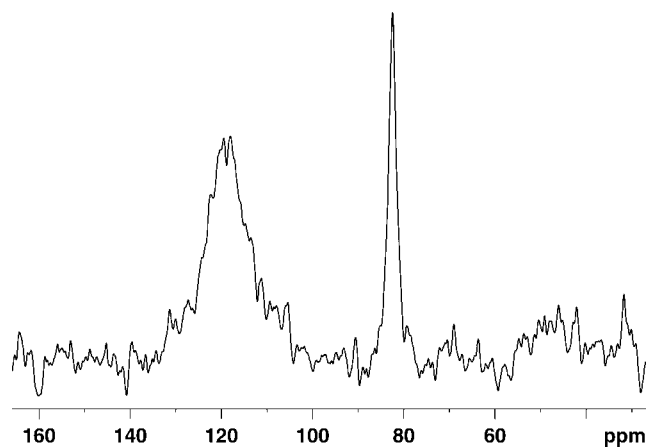


Figure 5. ^{15}N CP/MAS spectrum of 572 nmol almond β -glucosidase in complex with 0.9 equiv. **1b**. The spectrum was recorded using 12000 scans, 5 kHz spinning, 1 ms CP contact time, and a 4 s relaxation delay.

ment.^[18] Solid and dashed lines in Figure 6 represents fits of the experimental data (+) to NH and NH_2 spin systems, respectively. For ^{15}N -*t*-Boc-valine, **1b**, and protein backbone, fits to an NH spin system (rmsd values of 0.11, 0.15, and 0.21) are clearly better than fits to an NH_2 spin system (rmsd values of 0.99, 0.50, and 0.36), consistent with the known structure for all three compounds. The shown NH curves correspond to T_{IS} values of 46, 64, and 54 μs and T_d values of 787, 535, and 1032 μs . We note that these values are in the same range for the three NH compounds. For the **1b**- β -glucosidase complex, iterative fitting to the NH and NH_2 models result in relatively higher rmsd values of 0.47 and 0.44, with optimized T_{IS} values of 48 and 60 μs and T_d values of 0.998 and 99.2 ms, respectively.

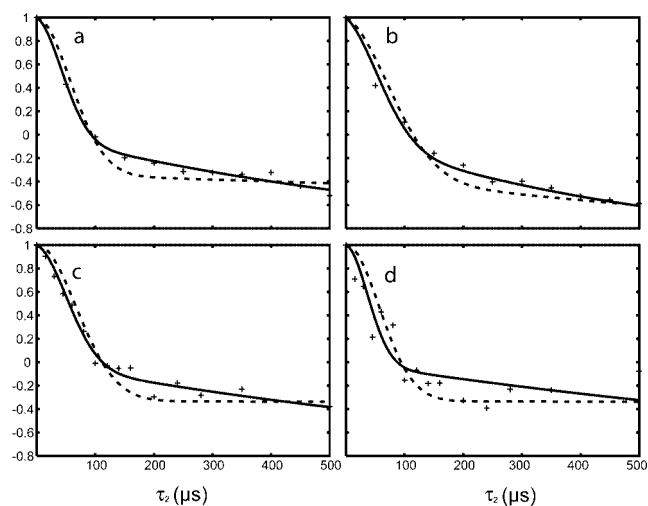


Figure 6. ^{15}N CPD/MAS depolarization data points (+) for a) ^{15}N -*t*-Boc-valine, b) **1b**, c) natural abundance protein backbone, and d) **1b**- β -glucosidase complex. Data in a) were acquired at room temperature, while those of b)–d) were recorded at -21°C . The experiments used 5 kHz spinning, 1 ms CP contact time, and 80 kHz SPINAL64^[21] decoupling. Solid and dashed lines illustrate best fits to NH and NH_2 groups, respectively.

$$I_{IS}(\tau_2) = \exp\left\{\frac{-\tau_2}{T_d}\right\} + \exp\left\{-\frac{1}{2}\left(\frac{3\tau_2}{T_d} + \left(\frac{\tau_2}{T_2}\right)^2\right)\right\} - 1 \quad (1)$$

$$I_{IS}(\tau_2) = \frac{2}{3}\left[\exp\left\{\frac{-\tau_2}{T_d}\right\} + 2\exp\left\{-\frac{1}{2}\left(\frac{3\tau_2}{T_d} + \left(\frac{\tau_2}{T_2}\right)^2\right)\right\}\right] - 1 \quad (2)$$

Symmetry-based $\text{R}18^{71}$ and $\text{R}18^{52}$ pulse sequences were also considered in order to determine the protonation extend of the nitrogens. An R18 sequence applied on the ^1H decoupling channel during acquisition on the ^{15}N channel allows recoupling of the heteronuclear ^1H - ^{15}N dipolar coupling combined with homonuclear ^1H decoupling. The ^{15}N spectrum is therefore highly dependent on the protonation, and large splittings of the signals are observed. However, conclusions on the protonation could not be drawn from the obtained spectra of the **1b**-glucosidase complex due to large overlaps between the broad – and now also split – backbone signals and the signal of the isotope labelled 2- ^{15}N site. Low signal-to-noise ratio in the spectra also hampered these types of experiments.

Discussion. The inhibition profiles at variant pH show not only that the inhibition of α - and β -glucosidase by **1** is dependent on pH, but also that protonation of the inhibitor is important for the inhibition, since if **1** and 1H^+ bound equally well, the inhibition curve would be identical to the k_{cat}/K_m curve. For both enzymes, the data are consistent with **1** binding EH or 1H^+ binding E (or a combination) and since the latter possibility requires that the inhibitor is considerably stronger than the observed K_i (because little E and 1H^+ are present at optimum pH) it may appear less likely. In any case these results show that the bound inhibitor enzyme complex contains only one proton, the position of which, on the inhibitor or on the enzyme, can be a result of proton exchange upon binding.

The ^{13}C chemical shifts of **1a** bound to α -glucosidase and glucoamylase are remarkably similar, while the β -glucosidase signal is shifted significantly. This strongly suggests a different mode of binding in the two cases. Furthermore, the two former shifts are very similar to the chemical shift of **1a** in neutral solution ($\delta = 63.5$ ppm), indicating that the bound form of **1a** in α -glucosidase and glucoamylase is uncharged **1a**. On the other hand, the relatively low chemical shift of **1a** bound to β -glucosidase is much closer to that of **1a** in acidic solution ($\delta = 61.7$ ppm) suggesting that the inhibitor is protonated in β -glucosidase. Since **1** in acidic solution is a 2:1 mixture of the N1- and N2-protonated species so that the chemical shift of 61.7 ppm is an average of the two forms, and since protonation of amines mainly give an upfield shift in the β -position,^[22] the low value observed in β -glucosidase ($\delta = 60.2$ ppm) is strongly indicative of exclusive protonation at N1. A disruptive effect could, however, be caused by an enzyme specific through-space influence on the chemical shift, e.g., through ring current effect from an adjacent aromatic structural element.

From the ^{15}N chemical shift data in Table 2, calculated chemical shifts of hypothetical pure 1- and 2-protonated species are 72.1 and 84.1 ppm (taking the 2:1 1- to 2-protonation rate into account). 84.1 ppm is close to both the value of non-protonated **1b**, 85.3 ppm, and to the measured shift for β -glucosidase-bound **1b**, 82.6 ppm. It is evident that the ^{2-15}N chemical shift does not change significantly either upon protonation, or enzyme binding (where protonation is not expected). The latter fact suggests indirectly that the ^{13}C chemical shift changes upon binding are not governed by ring current effect of aromatic side chains, a possible concern for an enzyme with unknown structure, and therefore unknown side chain composition in the active site.

The ^{15}N CPD experiments were anticipated to be suitable for distinguishing between different protonation states of enzyme-bound inhibitors. It turns out, however, that by using current models for depolarization in IS and I₂S spin systems (here NH and NH₂ groups), it is not possible to unambiguously distinguish the two protonation models, although the expected NH model seems to give a slightly better fit than NH₂, and is described by more realistic spin diffusion constants. The lack of conclusive information may partly be due to a relatively low signal-to-noise ratio for ^{15}N labelled azafagomine in the enzyme binding site.

Nevertheless, the chemical shift measurements are altogether consistent with protonation occurring at N1 in β -glucosidase, while a different situation, either no protonation, or protonation at N2, exists in α -glucosidase. Since **1** is unprotonated at the pH of the NMR experiment it is clear that β -glucosidase induces protonation in the active site. This also means that the enzyme stabilizes the charged form of the inhibitor more than the neutral form. Such stabilizing interactions may also be used by the enzyme, in this case almond β -glucosidase, to stabilize a charged transition state relative to a neutral ground state. The results indicate that the bound form of **1a** is protonated at N1, which suggest that this enzyme stabilizes charge at the anomeric position.

Conclusion

The solid-state ^{13}C NMR results show that the inhibitor **1a** changes the chemical shifts in β -glucosidase, while it does not when bound to α -glucosidase and glucoamylase. Since ^{15}N NMR results reveal that no ring-current or similar effects from the protein are influencing the ^{15}N chemical shift significantly in β -glucosidase the ^{13}C chemical shift change strongly suggest that the inhibitor is protonated at N1 in β -glucosidase but not in the other enzymes. This means that the β -glucosidase active site stabilizes the protonated form of the inhibitor and consequently that it must also stabilize formation of positive charge in the substrate; this appears to be at the anomeric position (N1) rather than at the ring-oxygen position (N2).

Experimental Section

General: Solvents were distilled under anhydrous conditions. All reagents were used as purchased without further purification. Evaporation was carried out on a rotary evaporator with the temperature kept below 40 °C. Glassware used for water-free reactions was dried min. 2 h at 130 °C before use. Columns were packed with silica gel 60 (230–400 mesh) as the stationary phase. TLC plates (Merck, 60, F₂₅₄) were visualized by spraying with cerium sulfate (1%) and molybdic acid (1.5%) in 10% H₂SO₄ and heating till coloured spots appeared. ^1H -NMR, ^{13}C -NMR and COSY were carried out on a Varian Mercury 400 instrument. Chemical shifts are given in ppm and referenced to internal SiMe₄ (δ_{H} , δ_{C} = 0.00). J values are given in Hz. Mass spectra were obtained on a Micro-mass LCT-QTOF instrument. ^{13}C CP/MAS solid-state NMR spectroscopic data were recorded on a Varian Inova 400 MHz spectrometer using a 5 mm double-resonance VT MAS probe. The ^{15}N CP/MAS and CPD/MAS experiments were carried out using a Bruker 700 MHz Avance NMR spectrometer using a 4 mm triple-resonance MAS probe.

2,3,5-Tri-*O*-benzyl-L-xylono-1,4-lactone (3): To the solution of **2** (328 mg, 0.78 mmol) in dichloromethane (2 mL) was added solution of PCC (288 mg, 1.30 mmol) and Celite (288 mg) in dichloromethane (5 mL). This mixture was stirred overnight at room temperature. The solution was filtered through Celite, concentrated and subjected to flash chromatography (pure pentane to pentane:Et₂O, 7:3) to give **3** (308 mg, 95%), as a colorless oil. MS (ES): m/z 441.1667 [$M + \text{Na}$]⁺. C₂₆H₂₆O₅Na m/z 441.1672. ^1H NMR (CDCl₃): δ = 7.42–7.21 (m, 15 H, CH_{Ph}), 5.05 (d, 1 H, J_{gem} = 11.2 Hz, *H*-CHPh), 4.68 (d, 1 H, J_{gem} = 11.2 Hz, *H*-CHPh), 4.65 (d, 1 H, J_{gem} = 11.6 Hz, *H*-CHPh), 4.63–4.52 (m, 5 H, CH₂Ph, 4-H, 2-H), 4.37 (t, 1 H, J = 7.2 Hz, 3-H), 3.76 (dd, 1 H, J = 2.8 Hz, J_{gem} = 10.8 Hz, 5a-H), 3.72 (dd, 1 H, J = 3.6 Hz, J_{gem} = 10.8 Hz, 5b-H).

2,3,5-Tri-*O*-benzyl-L-xylonic Amide (4): Compound **3** (309 mg, 0.74 mmol) was dissolved in saturated solution of ammonia in methanol (8 mL). After stirring overnight, under N₂, the reaction mixture was concentrated to give **4** (320 mg, 99%), as a white solid. MS (ES): m/z : 458.1952 [$M + \text{Na}$]⁺. C₂₆H₂₉O₅NNa m/z 458.1943. ^{13}C NMR (CDCl₃): δ = 174.1 (C=O), 138.2, 138.1, 136.9 (C_{ipso}), 128.9–128.0 (CH_{Ph}), 81.1, 80.4, 77.6, 75.6, 73.9, 73.6, 70.8, 70.7. ^1H NMR (CDCl₃): δ = 7.32–7.15 (m, 15 H, CH_{Ph}), 4.81–4.32 (m, 6 H, CH₂Ph), 4.12 (d, 1 H, J = 4.4 Hz, 2-H), 4.05–4.02 (m, 1 H, 4-H), 3.93 (t, 1 H, J = 4.4 Hz, 3-H), 3.47 (dd, 1 H, J = 5.6 Hz, J_{gem} = 9.6 Hz, 5a-H), 3.42 (dd, 1 H, J = 6 Hz, J_{gem} = 9.6 Hz, 5b-H), 3.21 (br. d, 1 H, OH).

1-Amino-1-deoxy-2,3,5-tri-*O*-benzyl-L-xylitol (5): Compound **4** (344 mg, 0.79 mmol) was dissolved in THF (10 mL) under N₂ at room temperature. Lithium aluminum hydride (150 mg, 3.96 mmol) was then cautiously added. The reaction mixture was refluxing for next 7 h. The mixture was quenched by slowly addition of ethyl acetate, water (0.5 mL), 15% NaOH (0.5 mL) and water (1.3 mL). The resulting homogeneous solution was filtered and the remaining organic layer was diluted with water and extracted with diethyl ether (3 × 20 mL). Combined organic layers were dried (MgSO₄), and concentrated. The residue was subjected to flash chromatography (pure EtOAc to EtOAc:MeOH, 1:1) to give **5** (290 mg, 86%), as a colorless oil. MS (ES): m/z 422.2159 [$M + \text{H}$]⁺. C₂₆H₃₂NO₄ m/z 421.2331. ^{13}C NMR (CDCl₃): δ = 138.4, 138.1, 137.9 (C_{ipso}), 128.8–127.8 (CH_{Ph}), 77.0, 76.6, 73.7, 73.2, 72.7, 71.1, 67.1, 39.4 (C-NH₂). ^1H NMR (CDCl₃): δ = 7.45–7.18 (m, 15 H, CH_{Ph}), 4.58–4.44 (m, 6 H, CH₂Ph), 4.06 (dt, 1 H, J = 1.2 Hz, J = 6.8 Hz, 4-H), 3.74 (dd, 1 H, J = 1.2 Hz, J = 6.0 Hz, 5a-H), 3.64–3.51 (m, 3 H,

2-H, 3-H, 5b-H), 3.25 (dd, 1 H, $J = 4.8$ Hz, $J_{\text{gem}} = 12.4$ Hz, 1a-H), 3.00 (dd, 1 H, $J = 2.8$ Hz, $J_{\text{gem}} = 12.4$ Hz, 1b-H).

1-(Acetylamino)-1-deoxy-2,3,5-tri-*O*-benzyl-L-xylitol (6): Compound **5** (400 mg, 0.95 mmol) was dissolved in methanol (25 mL) and acetic anhydride (6 mL) was added. The mixture was kept for 18 h at room temperature, then concentrated and subjected to flash chromatography (EtOAc) to give **6** (393 mg, 90%), as a slowly crystallizing, white solid. MS (ES): m/z 486.2256 [$M + \text{Na}$]⁺. $\text{C}_{28}\text{H}_{33}\text{NO}_5\text{Na}$ m/z 486.2256. ^{13}C NMR (CDCl_3): $\delta = 170.6$ (C=O), 138.2, 138.1, 138.0 (C_{ipso}), 129.3–128.0 (CH_{Ph}), 78.1, 76.8, 74.4, 73.5, 72.6, 71.5, 69.4, 39.2, 23.4 (CH_3). ^1H NMR (CDCl_3): $\delta = 7.28$ – 7.18 (m, 15 H, CH_{Ph}), 5.85 (br. s, 1 H, NH), 4.70–4.44 (m, 6 H, CH_2Ph), 4.05 (ddd, 1 H, $J = 2.6$ Hz, $J = 3.6$ Hz, $J = 6.0$ Hz, 4-H), 3.76–3.74 (m, 1 H), 3.62 (dd, 1 H, $J = 3.6$ Hz, $J_{\text{gem}} = 9.2$ Hz, 5a-H), 3.55 (dd, 1 H, $J = 2.6$ Hz, $J_{\text{gem}} = 9.2$ Hz, 5b-H), 3.48 (dd, 1 H, $J = 6.4$ Hz, $J_{\text{gem}} = 9.6$ Hz, 1a-H), 3.43 (dd, 1 H, $J = 6.0$ Hz, $J_{\text{gem}} = 9.6$ Hz, 1b-H), 3.35–3.29 (m, 1 H), 2.69 (br. s, 1 H, OH), 1.82 (s, 3 H, CH_3).

1-(Acetyl-nitroso-amino)-1-deoxy-2,3,5-tri-*O*-benzyl-L-xylitol (7): Compound **6** (1.0 g, 2.17 mmol) was dissolved in glacial acetic acid (1 mL) and acetic anhydride (5 mL) and cooled to -3 °C. Under vigorously stirring ^{15}N -sodium nitrite (379 mg, 5.43 mmol) was slowly added. Then the reaction mixture was stirred for 10 h at room temperature and subsequently poured over ice-water bath and extracted with diethyl ether (4×50 mL). Combined organic layers were washed with 5% NaHCO_3 several times until all acetic acid was removed, then washed with water, dried (MgSO_4) and concentrated. The residue was subjected to flash chromatography (pentane:Et₂O, 4:6) to give **7** (826 mg, 77%) as a yellow oil. MS (ES): m/z 516.2117 [$M + \text{Na}$]⁺. $\text{C}_{28}\text{H}_{32}^{15}\text{NNO}_6\text{Na}$ m/z 516.2127. ^{13}C NMR (CDCl_3): $\delta = 174.8$ (C=O), 138.3, 137.9, 137.8 (C_{ipso}), 128.7–127.8 (CH_{Ph}), 77.6, 74.7, 74.2, 73.5, 73.0, 71.5, 68.7, 39.3 ($\text{CH}_2\text{-N}$), 22.6 (CH_3). ^1H NMR (CDCl_3): $\delta = 7.41$ – 7.03 (m, 15 H, CH_{Ph}), 4.65–4.62, 4.47–4.36, 4.16–4.13 (m, 6 H, CH_2Ph), 4.23 (dd, 1 H, $J = 8.8$ Hz, $J_{\text{gem}} = 14.0$ Hz, 5a-H), 3.99 (ddd, 1 H, $J = 2.8$ Hz, $J = 6.0$ Hz, $J = 6.4$ Hz, 2-H), 3.78 (dd, 1 H, $J = 3.4$ Hz, $J_{\text{gem}} = 14.0$ Hz, 5b-H), 3.63 (ddd, 1 H, $J = 3.4$ Hz, $J = 5.2$ Hz, $J = 8.8$ Hz, 4-H), 3.61 (dd, 1 H, $J = 6.4$ Hz, $J_{\text{gem}} = 9.6$ Hz, 1a-H), 3.51 (dd, 1 H, $J = 2.8$ Hz, $J = 5.2$ Hz, 3-H), 3.42 (dd, 1 H, $J = 6.0$ Hz, $J_{\text{gem}} = 9.6$ Hz, 1b-H), 2.51 (s, 3 H, CH_3).

1-(Acetyl-nitroso-amino)-2,3,5-tri-*O*-benzyl-4-*O*-methylsulfonyl-L-xylitol (8): Compound **7** (820 mg, 1.66 mmol) was dissolved in pyridine (40 mL) and cooled to 0 °C. Methanesulfonyl chloride (162 μL , 2.09 mmol) was added and the reaction mixture was allowed to reach room temperature over 1.5 h. Water (20 mL) was added and the mixture was extracted with CH_2Cl_2 (2×20 mL). Finally the combined organic layers were concentrated by coevaporation with toluene. The residue was subjected to flash chromatography (pentane:Et₂O, 1:1) to give **8** (844 mg, 89%) as a yellow oil. MS (ES): m/z 594.1901 [$M + \text{Na}$]⁺. $\text{C}_{29}\text{H}_{34}^{15}\text{NNO}_8\text{SNa}$ m/z 594.1903. ^{13}C NMR (CDCl_3): $\delta = 174.9$ (C=O), 137.7, 137.6, 137.5 (C_{ipso}), 128.7–128.0 (CH_{Ph}), 80.7, 77.8, 74.9, 74.3, 73.5, 73.1, 67.0, 38.7 ($\text{CH}_2\text{-N}$), 38.4 (CH_3), 22.7 (CH_3). ^1H NMR (CDCl_3): $\delta = 7.38$ – 7.01 (m, 15 H, CH_{Ph}), 4.84–4.81 (m, 1 H, 4-H), 4.67–4.30 (m, 6 H, CH_2Ph), 4.03 (dd, 1 H, $J = 6.8$ Hz, $J_{\text{gem}} = 14.2$ Hz, 1a-H), 3.92 (dd, 1 H, $J = 4.4$ Hz, $J_{\text{gem}} = 14.2$ Hz, 1b-H), 3.66 (dd, 1 H, $J = 3.6$ Hz, $J_{\text{gem}} = 11.2$ Hz, 5a-H), 3.59–3.54 (m, 2 H, H-3, 2-H), 3.51 (dd, 1 H, $J = 6.8$ Hz, $J_{\text{gem}} = 11.2$ Hz, 5b-H), 2.95 (s, 3 H, CH_3), 2.53 (s, 3 H, CH_3).

(3*R*,4*R*,5*R*)-1-Acetyl-4,5-bis(benzyloxy)-3-(benzyloxymethyl)hexahydropyridazine (9): Titanium(IV) chloride (159 μL , 1.45 mmol) was slowly added under N_2 to the solution of dichloromethane and

diethyl ether (4:1, 10 mL). Magnesium turnings (34.8 mg, 1.45 mmol) were added and the reaction mixture was stirred at room temperature for 3 h. After cooling to -5 °C ethereal solution of nitroso compound **8** (208 mg, 0.36 mmol) was added to the black suspension and stirred for 10 min. Hydrochloric acid (0.3 M, 0.4 mL) was added, and reaction was stirred for another 25 min at room temperature. The reaction mixture was made alkaline by addition of diluted NaOH, filtered through Celite and extracted with dichloromethane (100 mL). The organic phase was washed with brine, dried (MgSO_4) and concentrated. This residue was dissolved in nitromethane (10 mL), EtN(*i*Pr)₂ (1.1 mL, 6.32 mmol) was added, and the mixture was heated at 60 °C for 18 h. The solvent was evaporated, and the residue was subjected to flash chromatography (pure CH_2Cl_2 to CH_2Cl_2 :EtOAc, 1:4) to give **9** (347 mg, 53%) as a colorless oil. MS (ES): m/z 462.2591 [$M + \text{H}$]⁺. $\text{C}_{28}\text{H}_{33}^{15}\text{NNO}_4$ m/z 462.2409. ^{13}C NMR (CDCl_3): $\delta = 173.0$ (C=O), 138.6, 138.2, 137.9 (C_{ipso}), 128.7–127.9 (CH_{Ph}), 78.0, 74.9, 73.6 (2C), 72.2, 67.2, 60.6, 45.0, 20.8 (CH_3); ^1H NMR (CDCl_3): $\delta = 7.29$ – 7.12 (m, 15 H, CH_{Ph}), 4.79 (d, 1 H, $J_{\text{gem}} = 11.2$ Hz, $H\text{-CHPh}$), 4.66 (d, 1 H, $J_{\text{gem}} = 11.2$ Hz, $H\text{-CHPh}$), 4.72–4.65 (m, 1 H), 4.53 (d, 1 H, $J_{\text{gem}} = 11.2$ Hz, $H\text{-CHPh}$), 4.47 (d, 1 H, $J_{\text{gem}} = 11.2$ Hz, $H\text{-CHPh}$), 4.39 (d, 1 H, $J_{\text{gem}} = 11.2$ Hz, $H\text{-CHPh}$), 4.29 (d, 1 H, $J_{\text{gem}} = 11.2$ Hz, $H\text{-CHPh}$), 3.73 (ddd, 1 H, $J = 3.2$ Hz, $J = 5.6$ Hz, $J = 9.0$ Hz), 3.68 (t, 1 H, $J = 8.2$ Hz), 3.63–3.57 (m, 2 H), 2.83–2.67 (m, 2 H), 2.08 (s, 3 H, CH_3).

2- ^{15}N -(3*R*,4*R*,5*R*)-4,5-Dihydroxy-3-(hydroxymethyl)hexahydropyridazine [(–)-2- ^{15}N -labelled-azafagomine, **1b]:** To a solution of **9** (290 mg, 0.63 mmol) in EtOH (15 mL) was added HCl (1 M, 4.2 mL) and Pd/C (126 mg) and the solution was hydrogenated at 1 atm H_2 until all starting material disappeared (4–5 h). The mixture was filtered through Celite and concentrated to give a residue containing (3*R*,4*R*,5*R*)-1-acetyl-4,5-dihydroxy-3-(hydroxymethyl)-hexahydropyridazine. This was dissolved in HCl (6 M, 15 mL) and heated to 100 °C for 18 h. The solution was concentrated and subjected to ion-exchange chromatography using Amberlite IR-120 resin (H^+ , 10 mL) and eluting with diluted NH_4OH solution (150 mL). Concentration of alkaline eluate gave **1b** (55 mg, 59%) as a solid. MS (ES): m/z 150.0849 [$M + \text{H}$]⁺. $\text{C}_5\text{H}_{13}^{15}\text{NNO}_3$ m/z 150.0895. ^{13}C NMR (D_2O): $\delta = 72.0$, 71.6, 63.1, 59.7, 51.8. ^1H NMR (D_2O): $\delta = 3.71$ (ddd, 1 H, $J = 5.6$ Hz, $J = 9.6$ Hz, $J = 10.8$ Hz, 2-H), 3.56 (dd, 1 H, $J = 3.2$ Hz, $J_{\text{gem}} = 10.4$ Hz, 5a-H), 3.47 (dd, 1 H, $J = 6$ Hz, $J_{\text{gem}} = 10.4$ Hz, 5b-H), 3.21 (t, 1 H, $J = 9.6$ Hz, 3-H), 3.06 (dt, 1 H, $J = 5.6$ Hz, $J_{\text{gem}} = 12.8$ Hz, 1a-H), 2.55 [dddd, 1 H, $J = 1.1$ Hz (^{15}N - ^1H), $J = 3.2$ Hz, $J = 6.0$ Hz, $J = 9.6$ Hz, 4-H], 2.45 (dd, 1 H, $J = 10.8$ Hz, $J_{\text{gem}} = 12.8$ Hz, 1b-H); ^{15}N NMR (D_2O): $\delta = 83.1$ ppm.

Supporting Information (see also the footnote on the first page of this article): Figure S1 and S2 showing curves of k_{cat}/K_m for α - and β -glucosidases (2 pages) are available.

Acknowledgments

This work has been supported by the Danish Biotechnological Instrument Center, Carlsberg Fonden, the Lundbeck Foundation, Novo Nordisk fonden, the Danish Natural Science Foundation and the Danish National Research Foundation. We are grateful to Anne Bülow for assistance with sample preparation.

[1] J. Alper, *Science* **2001**, *291*, 2338–2343.

[2] L. Pauling, *Am. Sci.* **1948**, *36*, 51–58.

[3] N. Asano, R. J. Nash, R. J. Molyneux, G. W. J. Fleet, *Tetrahedron: Asymmetry* **2000**, *11*, 1645–1680.

- [4] V. Lillelund, X. Liang, H. H. Jensen, M. Bols, *Chem. Rev.* **2002**, *102*, 515–553.
- [5] G. W. J. Fleet, *Tetrahedron Lett.* **1985**, *26*, 5073–5076.
- [6] M. Bols, *Acc. Chem. Res.* **1998**, *31*, 1–8.
- [7] A. Varrot, M. Schuelein, M. Pipelier, A. Vasella, G. J. Davies, *J. Am. Chem. Soc.* **1999**, *121*, 2621–2622.
- [8] A. Varrot, C. A. Tarling, J. M. MacDonald, R. V. Stick, D. L. Zechel, S. G. Withers, G. J. Davies, *J. Am. Chem. Soc.* **2003**, *125*, 7496–7497.
- [9] T. M. Gloster, S. J. Williams, S. Roberts, C. A. Tarling, J. Wicki, S. G. Withers, G. J. Davies, *Chem. Commun.* **2004**, 1794–1795.
- [10] R. Hoos, A. B. Naughton, W. Thiel, A. Vasella, K. Rupitz, S. G. Withers, *Helv. Chim. Acta* **1993**, *76*, 2666–2686.
- [11] A. Berger, M. Ebner, A. E. Stuetz, *Tetrahedron Lett.* **1995**, *36*, 4989–4990.
- [12] M. Bols, R. G. Hazell, I. B. Thomsen, *Chem. Eur. J.* **1997**, *3*, 940–947.
- [13] B. V. Ernholz, I. B. Thomsen, A. Lohse, I. Plesner, K. B. Jensen, R. G. Hazell, X. Liang, A. Jacobsen, M. Bols, *Chem. Eur. J.* **2000**, *6*, 278–287.
- [14] The enzymes were yeast α -glucosidase (Fluka, 63 kDa, 66 U/mg), almond β -glucosidase (Sigma, 135 kDa, 25 U/mg) and *Aspergillus niger* glucoamylase (Sigma, 80 kDa, 40 U/mg) for which we have calculated a purity of 75, 95, and 67%, respectively, by assuming one active site.
- [15] S. U. Hansen, I. W. Plesner, M. Bols, *ChemBioChem* **2000**, *1*, 177–180.
- [16] A. García-Herrero, E. Montero, J. L. Muñoz, J. F. Espinosa, A. Vián, J. L. García, J. L. Asensio, F. J. Cañada, J. Jiménez-Barbero, *J. Am. Chem. Soc.* **2002**, *124*, 4804–4810.
- [17] J. F. Espinosa, E. Montero, A. Vian, J. L. García, H. Dietrich, R. R. Schmidt, M. Martín-Lomas, A. Imberty, F. J. Cañada, J. Jiménez-Barbero, *J. Am. Chem. Soc.* **1998**, *120*, 1309–1318.
- [18] In this study (\pm)-**1a** was used, which practically means (–)-**1a** because the corresponding (+)-form is a very weak inhibitor ($K_i \gg 1$ mM) of these enzymes.
- [19] S. U. Hansen, M. Bols, *J. Chem. Soc., Perkin Trans. 1* **1999**, 3323–3325.
- [20] R. Sangill, N. Rastrup-Andersen, H. Bildsøe, H. J. Jacobsen, N. C. Nielsen, *J. Magn. Reson. Ser. A* **1994**, *107*, 67–78.
- [21] B. M. Fung, A. K. Khitin, K. Ermolaev, *J. Magn. Reson.* **2000**, *142*, 97–101.
- [22] E. Pretch, W. Simon, J. Seibl, T. Clerc, Tables of Spectral Data for Structure Determination of Organic Compounds, Springer, Berlin, **1989**.

Received: September 19, 2006

Published Online: December 12, 2006